Pergamon

Int. J. Heat Mass Transfer. Vol. 38, No. 18, pp. 3369–3383, 1995

0017–9310/95 $9.50+0.00

0017–9310(95)00091–7

Mass exchange between droplets during head-on collisions of multisize sprays

F. ANIDJAR, Y. TAMBOUR† and J. B. GREENBERG

Faculty of Aerospace Engineering, Technion—Israel Institute of Technology, Haifa 32000, Israel

(*Received* 22 *June* 1994 *and in final form* 16 *February* 1995)

Abstract—A derivation of sectional equations for mass exchange between colliding droplets during head-on collisions of multisize (polydisperse) sprays is presented. The collision terms of these equations account for binary collisions which lead to coalescence and immediate break-up into two new droplets which differ in mass from the original droplets. That is, mass is exchanged between the original droplets. The amount of exchanged mass is allowed to vary between 0 and 100% of the mass of the donor droplet. The new equations are employed here to analyze the time evolution in droplet size distributions of two head-on colliding polydisperse sprays.

1. INTRODUCTION

In pioneering experimental studies carried out by Ashgriz and Poo [1] (see also Ashgriz and Givi [2, 3]), and independently by Jiang *et al.* [4], evidence has been provided for the phenomenon of mass exchange between droplets during head-on collisions. For example, Ashgriz and Poo [1] presented frame by frame color photographs showing a 'large' red droplet colliding with a smaller white droplet. The two droplets coalesce, and immediately separate and form two new droplets, a new red droplet, smaller in size, and a larger pink droplet.

Thus, in the case of collisions between two multisize (polydisperse) sprays, mass exchange between droplets occurs. At each time instant, the overall size distribution of droplets in the arena where the collisions take place is comprised of a combination of droplets (from the two original sprays) which have not participated in collisions and the newly formed droplets which have exchanged mass between them.

The purpose of the present study is to analyze the evolution in the overall droplet size distribution and the evolution in size distributions of the two colliding sprays. To perform this task, we first present a new derivation of sectional equations for mass exchange between droplets, then we present time-dependent solutions of these equations for two polydisperse sprays of arbitrary size distribution which are involved in head-on collisions.

The conditions under which droplets coalesce have been analyzed by various researchers (e.g. refs. [5–7], to cite just a few contributions). Thus, for the sake of generality, inertial coalescence of droplets is also accounted for in the present study. The above terminology applies to coalescence due to collisions between droplets that travel in the same direction with slightly different speeds [8–11]. Experimental evidence for the occurrence of inertial coalescence was provided by Yule *et al.* [12] who presented data for the downstream evolution in drop-size histograms indicating that large droplets that do not exist at upstream stations are detected further downstream. An independent theoretical simulation [8] of the downstream evolution of local drop-size distributions in which coalescence effects were taken into account agreed well with the above-described experimental results, thus supporting the hypothesis of inertial droplet coalescence in decelerating flows. Since the mathematical treatment of inertial coalescence via a sectional approach is well documented [8–11, 13, 14] and widely applied [8, 15, 16], it will not be repeated in the present study. Thus, as stated above, we shall focus here only on the derivation of new sectional equations for mass exchange between droplets during head-on collisions.

2. SECTIONAL EQUATIONS FOR MASS EXCHANGE BETWEEN DROPLETS

We consider a small control volume in which collisions between droplets of two opposing sprays take place (the schematic description is given in Fig. 1). Next, let us assume that one spray consists of red droplets whereas the other spray consists of blue droplets. Each spray is polydisperse (i.e. multisize) and has a discrete size distribution: $n_{i(r)}$ for the 'red' spray and $n_{i(b)}$ for the 'blue' spray. Here, n_i is the number density of i-mer droplets, i.e. of droplets consisting of an integer number of monomers i, where a monomer is a basic mass unit, e.g. a mass of a droplet 1 μm in diameter.

The rate of change of the number concentration of the 'red' i-mer droplets, due to collisions with 'blue'

†Author to whom correspondence should be addressed.

NOMENCLATURE

a strain rate
$B_{l,l+1}$ sectional evaporation coefficient, accounting for droplets from section $l+1$ that are added to section l during their evaporation
C_l sectional evaporation coefficient, accounting for evaporation of droplets within section l and of droplets that 'move' from section l to section $l-1$
D_m non-dimensional Damkohler-like numbers defined by equations (39)–(41)
E evaporation rate
E_i frequency of losing a monomer from an i-mer droplet by evaporation
i mass of an i-mer droplet in terms of number of monomers
j mass of a j-mer droplet in terms of number of monomers
k_l number of monomers in the largest droplet in section l
$k_{l-1}+1$ number of monomers in the smallest droplet in section l
l drop-size section l, bounded by the upper and lower limits L_l and U_l, respectively
L_l lower limit of drop-size in section l
m number of drop-size sections
$\tilde{m}_1$ mass of a single monomer, also mass of a droplet of the size of a single monomer
n_i number density of i-mer droplets
$n_{i(\mathrm{b})}$ number density of 'blue' i-mer droplets
$n_{i(\mathrm{r})}$ number density of 'red' i-mer droplets
p mass of a 'purple' droplet in terms of number of monomers
p' a fraction of the mass of a 'purple' droplet
p'' conjugate fraction of the mass of a 'purple' droplet
q a general property of the spray, see equation (8), may represent: number density, or mass density, or surface area density of the spray upon the proper choice of the coefficients α and γ
Q_l integral property of the spray within the lth drop-size section, see equation (11), may represent: number density, or mass density, or surface area density of the spray upon the proper choice of the coefficients α and γ
Q_{total} sum of Q values of all drop size sections
r radius of a colliding droplet
$\dot{S}^{\mathrm{I.C.}}$ source term, representing droplets subtracted from or added to a group of droplets of a kind described by an index appended to the source term notation
t time
u relative velocity at impact between colliding drops and the host gas fluid
U_l upper limit of drop-size in section l
$\tilde{v}_1$ volume of a single monomer, also volume of a droplet the size of a single monomer
We Weber number, see equation (43)
x length dimension of control volume.

Greek symbols

α a coefficient whose value determines (together with the proper choice for γ) the nature of the general spray property q and the integral property Q; for $\alpha = \alpha_{\mathrm{n}} = 1$ the above properties are number densities, for $\alpha = \alpha_{\mathrm{v}} = \tilde{v}_1$ (or $\tilde{m}_1$), they are volume (or mass) densities, and for $\alpha = \alpha_{\mathrm{s}} = \pi^{1/3}6^{2/3}\tilde{v}_1^{2/3}$ they are surface area densities
$\beta_{i(\mathrm{r}),j(\mathrm{b})}$ collision frequency between a 'red' i-mer droplet and a 'blue' j-mer droplet
$\bar{\beta}(\mathrm{b})_{K(\mathrm{r})M(\mathrm{b})}$ sectional collision coefficient between 'red' droplets of section K and 'blue' droplets of section M, accounting for the reduction in the Q property of the 'blue' droplets of section M defined by equation (38)
$\bar{\beta}(\mathrm{r})_{K(\mathrm{r})M(\mathrm{b})}$ sectional collision coefficient between 'red' droplets of section K and 'blue' droplets of section M, accounting for the reduction in the Q property of the 'red' droplets of section K defined by equation (37)
$\bar{\beta}_{K(\mathrm{r}),M(\mathrm{b}),l(\mathrm{p})}$ sectional collisional-formation coefficient, accounting for the formation of new 'purple' droplets in section $l(\mathrm{p})$ by collisions between 'red' droplets from section K and 'blue' droplets from section M, defined by equation (31)
γ a coefficient whose value determines (together with the proper choice for α) the nature of the general spray property q and the integral property Q; for $\gamma = \gamma_{\mathrm{n}} = 0$ the above properties are number densities, for $\gamma = \gamma_{\mathrm{r}} = 1$ (or $\tilde{m}_1$), they are volume (or mass) densities, and for $\gamma = \gamma_{\mathrm{s}} = 2/3$ they are surface area densities

η mass fraction of a donor droplet that is transferred to another droplet during collision ($0 < \eta \leqslant 1$)
θ(condition) condition function, see equation (17), which equals unity if the condition is satisfied or zero otherwise
ρ density of the liquid of which the droplets are comprised
σ surface tension
τ characteristic time.

Subscripts
i i-mer droplets; droplets consisting of an integer number of monomers i
i(b) i-mer droplet—'blue'
i(r) i-mer droplet—'red'
j j-mer droplets; droplets consisting of an integer number of monomers i
j(b) j-mer droplet—'blue'
j(r) j-mer droplet—'red'
K(r) section K—'red'
l(p) section l—'purple'
m the number of the highest section
M(b) section M—'blue'
LDS large droplet donates mass to a small droplet
SDL small droplet donates mass to a large droplet.

Superscripts
I.C. inertial coalescence, coalescence due to collisions between droplets which travel in the same direction with slightly different speeds.

droplets and due to evaporation can be described by the following set of coupled differential equations for $n_{1(r)}, n_{2(r)} \ldots$, etc.

$$\frac{d}{dt}n_{i(r)} = -n_{i(r)} \sum_{j(b)=1}^{\infty} \beta_{i(r),j(b)} n_{j(b)} \quad \text{collisions}$$
$$- E_{i(r)} n_{i(r)} + E_{i+1(r)} n_{i+1(r)} \quad \text{evaporation}$$
$$+ \dot{S}^{I.C.}_{i(r)} \quad \text{inertial-coalescence}$$
$$i(r) = 1, 2, 3 \ldots . \qquad (1)$$

In the above, $\beta_{i(r),j(b)}$ is the collision frequency between a 'red' i-mer droplet and a 'blue' j-mer droplet, and E_i is the frequency of losing a monomer from an i-mer droplet by evaporation. The source term $\dot{S}^{I.C.}_{(r)}$ represents inertial coalescence due to collisions between droplets of the 'red' spray which travel in the same direction with slightly different speeds. Explicit mathematical expressions for this source term appear in other publications [8, 11, 13, 14] and hence will not be repeated here. In the present study, we focus on

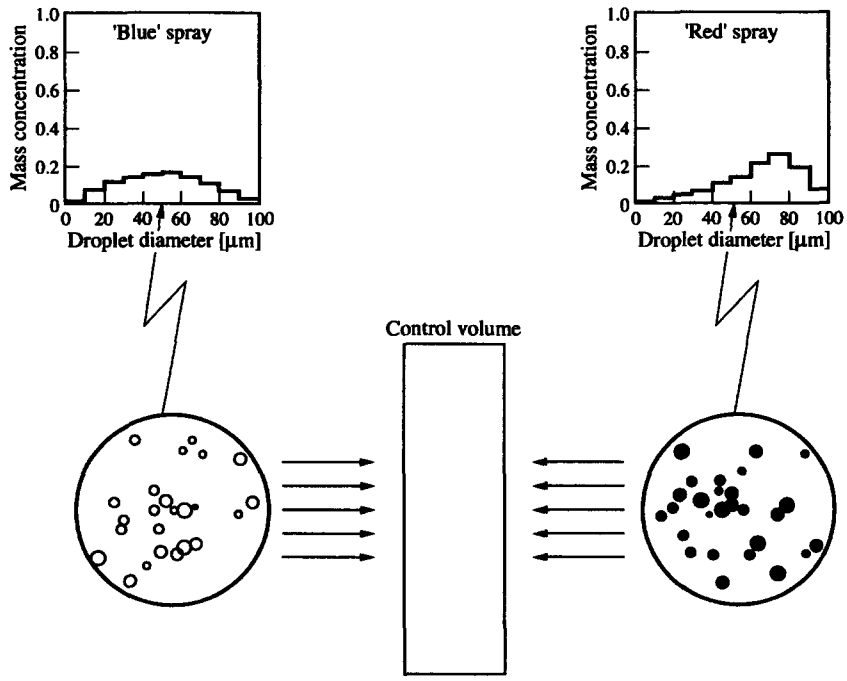

Fig. 1. Initial drop-size histograms of the 'blue' spray and the 'red' spray, and diagram of a head-on collision between the two sprays.

the mathematical derivation of the terms that are unique to head-on collisions. These are represented by the first term on the right-hand side of equation (1).

Similarly, the rate of change of the number concentration of the 'blue' i-mer droplets can be written as

$$\frac{\mathrm{d}}{\mathrm{d}t}n_{i(\mathrm{b})} = -n_{i(\mathrm{b})}\sum_{j(\mathrm{r})=1}^{\infty}\beta_{i(\mathrm{b}),j(\mathrm{r})}n_{j(\mathrm{r})} \quad \text{collisions}$$

$$-E_{i(\mathrm{b})}n_{i(\mathrm{b})}+E_{i+1(\mathrm{b})}n_{i+1(\mathrm{b})} \quad \text{evaporation}$$

$$+\dot{S}^{\mathrm{I.C.}}_{i(\mathrm{b})} \quad \text{inertial-coalescence}$$

$$i(\mathrm{b}) = 1, 2, 3 \ldots . \tag{2}$$

As a result of a collision between a 'red' droplet i(r) and a 'blue' droplet j(b), mass is exchanged between the two colliding droplets. The droplet that loses mass will be termed here the donor droplet. After losing mass, it will be called a 'purple' droplet, as it does not retain its pure original color, since during a collision the two colors of the colliding droplets partially blend before the separation of the newly formed droplets. Thus, these newly formed droplets will be termed 'purple' droplets and their 'mass' in terms of monomers will be denoted by p' and p''. If we denote by η the mass fraction of the donor droplet that is transferred to the other droplet, then if i donates to j:

$$p' = (1-\eta)i \tag{3}$$

$$p'' = j+\eta i \tag{4}$$

and in the case that j donates to i:

$$p' = (1-\eta)j \tag{5}$$

$$p'' = i+\eta j \tag{6}$$

where i and j denote the 'mass' in terms of monomers of the two colliding droplets. Note that i and j are integers, whereas p' and p'' may consist of fractions of monomers since the value of η can be any value between zero and unity, i.e.

$$0 < \eta \leqslant 1. \tag{7}$$

For example, the diameters of droplets before and after collision as they appear in photographs in the paper by Ashgriz and Poo [1] show for one of the cases mass exchange that corresponds approximately to $\eta = 0.82$. This is a fraction of the mass of the large droplet donated to the small droplet.

To account for changes in the surface area of droplets or the number density of droplets, we introduce a general property of the spray for each of the colliding droplets:

$$q_i(t) = \alpha i^{\gamma} n_i(t) \tag{8}$$

where i can be 'red' or 'blue', i.e.

$$i = i(\mathrm{r}) \text{ or } i(\mathrm{b}) \tag{9}$$

and since 'purple' droplets may consist of fractions of monomers, for a 'purple' droplet the general property q is defined as

$$q(p, t) = \alpha p^{\gamma} n(p, t) \tag{10}$$

where p represents both p' and p'' and $n(p, t)$ is a continuous number density function for the 'purple' droplets. It represents the number of 'purple' droplets in the size range between p and $p + \mathrm{d}p$, per unit volume, at time t.

In equations (8) and (10) the power γ is equal to zero, or unity, or $\gamma = 2/3$, depending on the property of interest. For example: for $\gamma_{\mathrm{n}} = 0$ and $\alpha_{\mathrm{n}} = 1$, q_i is simply equal to the number concentration $n_i(t)$; for $\gamma_{\mathrm{v}} = 1$, [and $\alpha_{\mathrm{v}} = \tilde{v}_1$ (or $\tilde{m}_1$), which is the volume (or mass) of a single monomer], q_i is the volume (or mass) of the i-mer droplets; and for $\gamma_{\mathrm{s}} = 2/3$ (and $\alpha_{\mathrm{s}} = \pi^{1/3}6^{2/3}\tilde{v}_1^{2/3}$), q_i is the surface area of the i-mer droplets.

Then, following refs. [8–11, 13, 14, 17–19], we divide the entire droplet size domain into m arbitrary sections; see Table 1. The spray is thus represented by bar-like drop-size histograms as measured by experimentalists [12, 20–23] at various spatial locations. Next we define $Q_l(t)$ to be an integral property of the spray within the lth section, that is

$$Q_l(t) = \sum_{i=L_l}^{U_l}\alpha i^{\gamma} n_i(t) \quad l = 1, 2, 3 \ldots, m \tag{11}$$

whereas for the continuous size distribution of 'purple' droplets, the summation in equation (11) is replaced by an integral

$$Q_{l(\mathrm{p})}(t) = \int_{L_{l(\mathrm{p})}}^{U_{l(\mathrm{p})}}\alpha p^{\gamma} n(p, t)\,\mathrm{d}p \tag{12}$$

where L_l and U_l denote the lower and upper bounds, respectively (of section l), i.e. they denote the number of monomers in the smallest and largest droplets, respectively, in the lth section. Here the limits of each lth section may be the same for each 'color' or one may divide the droplet-size spectrum of each color using a different division. Thus for the sake of generality, one may distinguish between the limits U_l and L_l for each color by allowing

$$l = l(\mathrm{r}) \text{ or } l(\mathrm{b}) \text{ or } l(\mathrm{p}). \tag{13}$$

The total number of sections may also be different for each 'color', i.e.

$$m = m(\mathrm{r}) \text{ or } m(\mathrm{b}) \text{ or } m(\mathrm{p}). \tag{14}$$

The newly formed 'purple' droplets are counted in the proper lth purple section, l(p), according to their size. That is, p' or p'' belong to section l if

Table 1. Sectional lower and upper limits given in terms of droplet diameters, initial drop-size distributions and sectional evaporation coefficients

Section no. j	Lower limit of section j L_j [μm]	Upper limit of section j U_j [μm]	Initial drop-size distributions ($t=0$) $\frac{Q_j}{Q_{\text{total}}}$ (blue)	$\frac{Q_j}{Q_{\text{total}}}$ (red)	Sectional evaporation coefficients $\frac{C_j}{E}$ [μm^{-2}]	$\frac{B_{j,j+1}}{E}$ [μm^{-2}]
1	1	10	0.020	0.010	4.133×10^{-2}	2.141×10^{-3}
2	10	20	0.080	0.020	8.568×10^{-3}	1.579×10^{-3}
3	20	30	0.120	0.030	3.947×10^{-3}	1.216×10^{-3}
4	30	40	0.140	0.050	2.432×10^{-3}	9.836×10^{-4}
5	40	50	0.155	0.095	1.721×10^{-3}	8.242×10^{-4}
6	50	60	0.160	0.130	1.319×10^{-3}	7.086×10^{-4}
7	60	70	0.135	0.190	1.063×10^{-3}	6.213×10^{-4}
8	70	80	0.105	0.245	8.876×10^{-4}	5.530×10^{-4}
9	80	90	0.065	0.175	7.604×10^{-4}	4.981×10^{-4}
10	90	100	0.020	0.055	6.642×10^{-4}	$0.000\times10^{+0}$

$$L_{l(\mathrm{p})} \leqslant p' \leqslant U_{l(\mathrm{p})} \tag{15}$$

or

$$L_{l(\mathrm{p})} \leqslant p'' \leqslant U_{l(\mathrm{p})}. \tag{16}$$

Thus, for later use we present the following discrete function

$$\theta\{\text{condition}\} = \begin{cases} = 1 \text{ if condition is satisfied} \\ = 0 \text{ otherwise.} \end{cases} \tag{17}$$

For example, in terms of this function, if p' belongs to section l(p)

$$\theta\{L_{l(\mathrm{p})} \leqslant p' \leqslant U_{l(\mathrm{p})}\} = 1. \tag{18}$$

Next, we write all the possible collisions between the 'red' droplets and 'blue' droplets as

$$\Sigma_{\mathrm{r}}\Sigma_{\mathrm{b}}\beta_{i(\mathrm{r}),j(\mathrm{b})}n_{i(\mathrm{r})}n_{j(\mathrm{b})} \tag{19}$$

where Σ_{r} and Σ_{b} stand for the summations over the whole range of sizes of the 'red' and 'blue' droplets, respectively. These summations can be rewritten as summations over all 'red' and 'blue' sections in the following way

$$\Sigma_{\mathrm{r}}\Sigma_{\mathrm{b}} = \sum_{K(\mathrm{r})=1}^{m(\mathrm{r})}\sum_{M(\mathrm{b})=1}^{m(\mathrm{b})}\left(\sum_{i(\mathrm{r})=L_{K(\mathrm{r})}}^{U_{K(\mathrm{r})}}\sum_{j(\mathrm{b})=L_{M(\mathrm{b})}}^{U_{M(\mathrm{b})}}\right) \tag{20}$$

which will be useful later. Here the summations within the brackets are carried out over all the 'red' droplets that belong to any section K(r) and over all the 'blue' droplets that belong to any section M(b). Then, one runs over all the 'red' sections by varying K(r) from K(r) = 1 up to the upper 'red' section m(r), and over all the 'blue' sections from M(b) = 1 up to m(b). This is expressed in equation (20) by the summations outside of the brackets.

Of all the above possible collisions between the 'red' and the 'blue' droplets, only those which form droplets p' and/or p'' that satisfy the conditions expressed by conditions (15) and/or (16) contribute mass to the lth 'purple' section l(p). Therefore, we employ the function θ [see equation (17)], in order to express the rate of change of the integral quantity $Q_{l(\mathrm{p})}$ as follows

$$\begin{aligned}\frac{\mathrm{d}}{\mathrm{d}t}Q_{l(\mathrm{p})} = \Sigma_{\mathrm{r}}\Sigma_{\mathrm{b}}[&\theta\{L_{l(\mathrm{p})} \leqslant p' \leqslant U_{l(\mathrm{p})}\}\alpha(p')^{\gamma} \\ &+\theta\{L_{l(\mathrm{p})} \leqslant p'' \leqslant U_{l(\mathrm{p})}\}\alpha(p'')^{\gamma}] \\ &\times\beta_{i(\mathrm{r}),j(\mathrm{b})}n_{i(\mathrm{r})}n_{j(\mathrm{b})} \\ &-C_{l(\mathrm{p})}Q_{l(\mathrm{p})}+B_{l,l+1(\mathrm{p})}Q_{l+1(\mathrm{p})} \\ &l(\mathrm{p}) = 1,2,3,\ldots,m(\mathrm{p}).\end{aligned} \tag{21}$$

The last two terms on the right-hand side of equation (21) represent evaporation of 'purple' droplets. Detailed derivation of these terms is given in previous publications [17, 18] and will not be repeated here. The first term expresses the decrease in Q_l due to the size reduction of evaporating droplets within section l and as a result of droplets that leave section l to join section $l-1$. However, due to evaporation of droplets in section $l+1$, droplets are added to section l. This is described by the second term. All the above effects are incorporated in the sectional evaporation coefficients C_l and $B_{l,l+1}$ (see refs. [17, 18]) that are given below in a discrete form which will be applicable later for treating evaporation of droplets within the sections of the 'red' and 'blue' sprays:

$$B_{l,l+1} = \left(\frac{k_l}{k_l+1}\right)^{\gamma}\frac{E_{k_l+1}}{k_{l+1}-k_l} \tag{22}$$

$$\begin{aligned}C_l = \left(\frac{k_{l-1}}{k_{l-1}+1}\right)^{\gamma}&\frac{E_{k_{l-1}+1}}{k_l-k_{l-1}}+\frac{1}{k_l-k_{l-1}} \\ &\times\sum_{i=k_{l-1}+1}^{k_l}\frac{1}{i^{\gamma}}E_i[i^{\gamma}-(i-1)^{\gamma}]\end{aligned} \tag{23}$$

where the number of monomers in the upper limit of section l, (U_l), is denoted by k_l and therefore the lower limit L_l consists of $k_{l-1}+1$ monomers. For the 'purple' spray which is treated in a continuous manner within each section, the above sectional evaporation coefficients are presented in the following continuous form [18]:

$$B_{l,l+1} = \left(\frac{U_l}{L_{l+1}}\right)^{\gamma} \frac{E(L_{l+1})}{U_{l+1} - U_l} \tag{24}$$

$$C_l = \left(\frac{U_{l-1}}{L_l}\right)^{\gamma} \frac{E(L_l)}{U_l - U_{l-1}} + \frac{1}{U_l - U_{l-1}} \int_{L_l}^{U_l} \frac{1}{v^{\gamma}} E(v)\, \mathrm{d}v^{\gamma}. \tag{25}$$

Numerical values for the above coefficients are listed in Table 1.

The contribution to Q_l of each newly formed 'purple' droplet is described in equation (21) by the terms $\alpha(p')^{\gamma}$ and $\alpha(p'')^{\gamma}$ which represent either mass or surface area or number density of droplets, depending on the property of interest [see equation (8)]. The mass values (in terms of monomers) for p' and p'' are functions of $i(\mathrm{r})$ and $j(\mathrm{b})$. Hence, the summations in equation (21) cannot be carried out without specifying the explicit mathematical descriptions for p' and p''. Nonetheless, we find it more convenient to proceed first with the mathematical sectional averaging of the summation terms in equation (21) and only later to specify p' and p''.

Thus, to carry out sectional averaging, we follow the procedures described in refs. [14, 18]. That is, in equation (21) we replace each n_i that belongs to any section K (or M) by an average value of the integral quantity Q_K (or Q_M). For example, for each 'red' i-mer droplet $i(\mathrm{r})$ that lies within the limits of section K, i.e. for

$$L_K \leqslant i(\mathrm{r}) \leqslant U_K \tag{26}$$

we take $n_{i(\mathrm{r})}$ to be

$$n_{i(\mathrm{r})} = \frac{Q_K}{\alpha[i(\mathrm{r})]^{\gamma}(U_K - L_K)}. \tag{27}$$

Similarly, for each 'blue' j-mer

$$L_M \leqslant j(\mathrm{b}) \leqslant U_M \tag{28}$$

$n_{j(\mathrm{b})}$ is replaced by

$$n_{j(\mathrm{b})} = \frac{Q_M}{\alpha[j(\mathrm{b})]^{\gamma}(U_M - L_M)}. \tag{29}$$

Then, substituting equation (27) and (29) into equation (21) finally leads to the following sectional equation for $Q_{l(\mathrm{p})}$

$$\frac{\mathrm{d}}{\mathrm{d}t} Q_{l(\mathrm{p})} = \sum_{K(\mathrm{r})=1}^{m(\mathrm{r})} \sum_{M(\mathrm{b})=1}^{m(\mathrm{b})} \times \bar{\beta}_{K(\mathrm{r}),M(\mathrm{b}),l(\mathrm{p})} Q_{K(\mathrm{r})} Q_M(b) \quad \text{collisional formation}$$
$$- C_{l(\mathrm{p})} Q_{l(\mathrm{p})} + B_{l(\mathrm{p}),l+1(\mathrm{p})} Q_{l+1(\mathrm{p})} \quad \text{evaporation}$$
$$l(\mathrm{p}) = 1, 2, \ldots, m(\mathrm{p}) \tag{30}$$

where the sectional collisional-formation coefficients $\bar{\beta}_{K(\mathrm{r}),M(\mathrm{b}),l(\mathrm{p})}$, which describe the formation of new 'purple' droplets in section $l(\mathrm{p})$ by collisions between 'red' droplets and 'blue' droplets from sections $K(\mathrm{r})$ and $M(\mathrm{b})$, respectively, can be expressed as

$$\bar{\beta}_{K(\mathrm{r}),M(\mathrm{b}),l(\mathrm{p})} = \sum_{i(\mathrm{r})=L_{K(\mathrm{r})}}^{U_{K(\mathrm{r})}} \sum_{j(\mathrm{b})=L_{M(\mathrm{b})}}^{U_{M(\mathrm{b})}} \times \frac{[\theta\{L_{l(\mathrm{p})} \leqslant p' \leqslant U_{l(\mathrm{p})}\}\alpha(p')^{\gamma} + \theta\{L_{l(\mathrm{p})} \leqslant p'' \leqslant U_{l(\mathrm{p})}\}\alpha(p'')^{\gamma}]}{\alpha^2[i(\mathrm{r})]^{\gamma}(U_{K(\mathrm{r})} - L_{K(\mathrm{r})})[j(\mathrm{b})]^{\gamma}(U_{M(\mathrm{b})} - L_{M(\mathrm{b})})} \beta_{i(\mathrm{r}),j(\mathrm{b})}$$
$$l(\mathrm{p}) = 1, 2, \ldots, m(\mathrm{p})$$
$$K(\mathrm{r}) = 1, 2, \ldots, m(\mathrm{r})$$
$$M(\mathrm{b}) = 1, 2, \ldots, m(\mathrm{b}). \tag{31}$$

A sample of the numerical values for the above coefficients is presented in Table 2.

As we have already mentioned, p' and p'' are functions of $i(\mathrm{r})$ and $j(\mathrm{r})$, and therefore one cannot carry out the summation in equation (31) before specifying the explicit mathematical descriptions for p' and p''. This task is performed next.

The mass value (in terms of monomers) for p' and p'' depends on whether the 'red' droplet is the donor or the 'blue' droplet is the donor. In Ashgriz and Poo's experiment [1], the larger droplet contributes mass to the smaller one. Thus, this case (which will be denoted by the subscript LDS, i.e. large donates to small) can be mathematically expressed, according to equation (3)–(6), as follows

Table 2. Sample of the numerical values for the head-on collision coefficients $\bar{\beta}_{K(\mathrm{r}),M(\mathrm{b})l(\mathrm{p})}$ for $\eta = 0.4$ and the case of large droplets that donate mass to small droplets, LDS, which were employed in our computations†

0	0	0	0	0	0	0	203.15	242.41	107.02
0	0	0	0	0	0	0	7.2812	8.9172	3.5599
0	0	0	0	0	0	0	1.7849	2.2228	0.6113
0	0	0	0	0	0	0	0.9731	0.9284	0.0689
0	0	0	0	0	0	0.1251	0.7354	0.3413	0
0	0	0	0	0	0.2370	0.3321	0.3855	0.0775	0
0	0	0	0	0.1251	0.3321	0.0610	0.1491	0.0502	0
203.15	7.2812	1.7849	0.9731	0.7354	0.3855	0.1491	0.1294	0.0369	0
242.41	8.9172	2.2228	0.9284	0.3413	0.0775	0.0502	0.0369	0.0088	0
107.02	3.5599	0.6113	0.0689	0	0	0	0	0	0

†Coefficients are normalized by a reference collision parameter $\beta_{\mathrm{ref}} = 0.13086$. The matrix given above is for $l(\mathrm{p}) = 7$ with $K(\mathrm{r}), M(\mathrm{b}) = 1, 2, 3 \ldots, 10$.

$$(p')_{\mathrm{LDS}} = \theta\{i(\mathrm{r}) \geqslant j(\mathrm{b})\}[(1-\eta)i(\mathrm{r})] + \theta\{j(\mathrm{b}) > i(\mathrm{r})\}[(1-\eta)j(\mathrm{b})] \quad (32a)$$

$$(p'')_{\mathrm{LDS}} = \theta\{i(\mathrm{r}) \geqslant j(\mathrm{b})\}[j(\mathrm{b})+\eta i(\mathrm{r})] + \theta\{j(\mathrm{b}) > i(\mathrm{r})\}[i(\mathrm{r})+\eta j(\mathrm{b})]. \quad (33a)$$

For the sake of generality, we also consider the possibility that small droplets will transfer mass to larger ones. In this case (which will be denoted by the subscript SDL), the inequality signs of the various θ functions in equations (32) and (33) will be reversed

$$(p')_{\mathrm{SDL}} = \theta\{i(\mathrm{r}) \leqslant j(\mathrm{b})\}[(1-\eta)i(\mathrm{r})] + \theta\{j(\mathrm{b}) < i(\mathrm{r})\}[(1-\eta)j(\mathrm{b})] \quad (32b)$$

$$(p'')_{\mathrm{SDL}} = \theta\{i(\mathrm{r}) \leqslant j(\mathrm{b})\}[j(\mathrm{b})+\eta i(\mathrm{r})] + \theta\{j(\mathrm{b}) < i(\mathrm{r})\}[i(\mathrm{r})+\eta j(\mathrm{b})]. \quad (33b)$$

Finally, we substitute equations (32) and (33) into equation (31) and employ the summations within the various sections to obtain $\bar{\beta}_{K(\mathrm{r}),M(\mathrm{b}),l(\mathrm{p})}$. Examples of numerical values obtained for these sectional collisional-formation coefficients, for a collision kernel

$$\beta_{i(\mathrm{r}),j(\mathrm{b})} = \beta([i(\mathrm{r})]^{2/3} + [j(\mathrm{b})]^{2/3}) \quad (34)$$

which represents an effective collisional cross-section area, are presented in Tables 2 and 3. Once these sectional collisional-formation coefficients are evaluated, solutions of the set of intercoupled sectional equations, equation (30), can be derived. These sectional solutions for the 'purple' droplets also depend on the evolution in droplet size distributions of the 'red' and 'blue' droplets which are presented by equation (1) and (2) in discrete forms. Thus, it is also necessary to re-express equation (1) and (2) in a sectional form. This yields the following sectional equations:

for 'red' droplets:

$$\frac{\mathrm{d}}{\mathrm{d}t}Q_{K(\mathrm{r})} = -Q_{K(\mathrm{r})}\sum_{M(\mathrm{b})=1}^{m(\mathrm{b})}\bar{\beta}(\mathrm{r})_{K(\mathrm{r}),M(\mathrm{b})}Q_{M(\mathrm{b})} \quad \text{collisions}$$
$$-C_{K(\mathrm{r})}Q_{K(\mathrm{r})} + B_{K(\mathrm{r}),K+1(\mathrm{r})}Q_{K+1(\mathrm{r})} \quad \text{evaporation}$$
$$+\dot{S}^{\mathrm{I.C.}}_{K(\mathrm{r})} \quad \text{inertial coalescence}$$
$$K(\mathrm{r}) = 1, 2, \ldots, m(\mathrm{r}) \quad (35)$$

for 'blue' droplets:

$$\frac{\mathrm{d}}{\mathrm{d}t}Q_{M(\mathrm{b})} = -Q_{M(\mathrm{b})}\sum_{K(\mathrm{r})=1}^{m(\mathrm{b})}\bar{\beta}(\mathrm{b})_{K(\mathrm{r}),M(\mathrm{b})}Q_{K(\mathrm{r})} \quad \text{collisions}$$
$$-C_{M(\mathrm{r})}Q_{M(\mathrm{b})} + B_{M(\mathrm{b}),M+1(\mathrm{b})}Q_{M+1(\mathrm{b})} \quad \text{evaporation}$$
$$+\dot{S}^{\mathrm{I.C.}}_{M(\mathrm{b})} \quad \text{inertial coalescence}$$
$$M(\mathrm{b}) = 1, 2, \ldots, m(\mathrm{b}). \quad (36)$$

In the above, the sectional-collision coefficients do not depend on the size of the newly formed 'purple' droplet [as in equation (31)]. Thus, all the θ conditions that appear in equation (31) will not be present in the sectional-collision coefficients of equation (35) and (36). The only contribution in equation (35) to the $Q_{k(\mathrm{r})}$ quantity due to a collision of each i-mer 'red' droplet will be a reduction in Q by $\alpha[i(\mathrm{r})]^{\gamma}$. Thus

$$\bar{\beta}(\mathrm{r})_{K(\mathrm{r}),M(\mathrm{b})} = \sum_{i(\mathrm{r})=L_{K(\mathrm{r})}}^{U_{K(\mathrm{r})}}\sum_{j(\mathrm{b})=L_{M(\mathrm{b})}}^{U_{M(\mathrm{b})}}\frac{\alpha[i(\mathrm{r})]^{\gamma}}{\alpha^2[i(\mathrm{r})]^{\gamma}(U_{K(\mathrm{r})}-L_{K(\mathrm{r})}) \times [j(\mathrm{b})]^{\gamma}(U_{M(\mathrm{b})}-L_{M(\mathrm{b})})}\beta_{i(\mathrm{r}),j(\mathrm{b})} \quad (37)$$

Table 3. Sample of the numerical values for the head-on collision coefficients $\beta(\mathrm{r})_{K(\mathrm{r}),M(\mathrm{b})}$ and $\beta(\mathrm{b})_{K(\mathrm{r})M(\mathrm{b})}$ which were employed in our computations†

	K	M			K	M		
$\beta(\mathrm{r})$	4,	1	=	$\beta(\mathrm{b})$	1,	4	=	84.127
$\beta(\mathrm{r})$	4,	2	=	$\beta(\mathrm{b})$	2,	4	=	3.3662
$\beta(\mathrm{r})$	4,	3	=	$\beta(\mathrm{b})$	3,	4	=	0.9212
$\beta(\mathrm{r})$	4,	4	=	$\beta(\mathrm{b})$	4,	4	=	0.4426
$\beta(\mathrm{r})$	4,	5	=	$\beta(\mathrm{b})$	5,	4	=	0.2753
$\beta(\mathrm{r})$	4,	6	=	$\beta(\mathrm{b})$	6,	4	=	0.1967
$\beta(\mathrm{r})$	4,	7	=	$\beta(\mathrm{b})$	7,	4	=	0.1526
$\beta(\mathrm{r})$	4,	8	=	$\beta(\mathrm{b})$	8,	4	=	0.1247
$\beta(\mathrm{r})$	4,	9	=	$\beta(\mathrm{b})$	9,	4	=	0.1055
$\beta(\mathrm{r})$	4,	10	=	$\beta(\mathrm{b})$	10,	4	=	0.0916

†Coefficients are normalized by a reference collision parameter $\beta_{\mathrm{ref}} = 0.13086$.

whereas the sectional-collision coefficient in the equation for the rate of change of $Q_{M(b)}$ will consist of a term $\alpha[j(b)]^{\gamma}$ in its numerator. That is

$$\bar{\beta}(b)_{K(r),M(b)} = \sum_{i(r)=L_{K(r)}}^{U_{K(r)}} \sum_{j(b)=L_{M(b)}}^{U_{M(b)}} \frac{\alpha[j(b)]^{\gamma}}{\alpha^2[i(r)]^{\gamma}(U_{K(r)}-L_{K(r)})[j(b)]^{\gamma}(U_{M(b)}-L_{M(b)})} \beta_{i(r),j(b)}. \tag{38}$$

A sample of the numerical values of the above coefficients is presented in Table 3.

Solutions of equation (30), (35) and (36) were carried out via a numerical integration. Results are presented in terms of non-dimensional Damkohler-like numbers for the head-on collision rates:

$$D_m(\text{collision}) = \frac{\tau_{\text{convection}}}{\tau_{\text{collision}}} \tag{39}$$

for the rate of evaporation:

$$D_m(\text{evaporation}) = \frac{\tau_{\text{convection}}}{\tau_{\text{evaporation}}} \tag{40}$$

and for the inertial coalescence rate:

$$D_m(\text{inertial coalescence}) = \frac{\tau_{\text{convection}}}{\tau_{\text{inertial coalescence}}} \tag{41}$$

where τ is a non-dimensional time

$$\tau_{\text{convection}} = \frac{1}{a} \tag{42}$$

where a is the strain rate.

3. RESULTS AND DISCUSSION

First we present results for the problem of mass transfer between the droplets of the two sprays ('blue' and 'red') due to collisions between droplets, but without evaporation. Mass histograms in Fig. 2(a)–(c) show the build-up with time of 'purple' droplets on account of the 'blue' and 'red' droplets. (Note that the time evolution is presented in our figures along a 'diagonal line' from the lower left corner to the upper right.)

When droplet evaporation is considered (see Fig. 3), the mass concentration of 'purple' droplets becomes much smaller than that of the previous case in which droplet evaporation was not included. The reasons for this behavior are twofold: first, some of the 'purple' droplets manage to evaporate; and second, evaporation hinders the rate of head-on collisions since the number and size of the colliding droplets are reduced by evaporation. [The reduction in size of the colliding droplets reduces the collisional cross-section area, see equation (34).]

On the other hand, the rate of head-on collisions is also the rate of 'destruction' of 'blue' and 'red' droplets. Thus, evaporation also hinders the rate of 'destruction' of 'red' and 'blue' droplets. Under certain operating conditions, this may lead to the following interesting, unexpected, result. That is, during head-on collisions, a non-evaporating spray may reach a lower concentration than that of an evaporating spray, since more droplets of the non-evaporating spray can be 'destroyed' by collisions. Compare, for example, the concentration of the non-evaporating 'red' spray of $\tau = 0.24$ (Fig. 2) with the concentration of the evaporating 'red' spray at $\tau = 0.28$ (Fig. 3).

When inertial coalescence of droplets within the 'red' spray and within the 'blue' spray are also considered in our computations, the various size spectra are shifted to the right. This is due to the creation of large droplets on account of smaller droplets that coalesce (see Fig. 4).

In Fig. 5, we compare the evolution in the overall ('blue'+'red'+'purple') mass concentration histograms for three different situations, namely: (a) head-on collisions only; (b) with evaporation; and (c) with evaporation and inertial coalescence. As expected, the overall mass concentration is drastically reduced due to evaporation of droplets irrespective of what may happen to droplets of a certain kind (see previous discussion of the evolution in concentration of 'red' non-evaporating droplets vs evaporating ones).

For case (a) in which only head-on collisions are considered, the overall size histogram shifts slightly to the left, since during the head-on collisions large droplets donate mass to small droplets. On the other hand in case (c), the creation of large droplets by coalescence of smaller droplets is noticeable.

When the conditions are such that large droplets donate 80% of their mass during head-on collisions (see, for example, our previous discussion of the experimental results presented by Ashgriz and Poo [1]), then the size histogram of the newly formed 'purple' droplets is flattened, also resulting in a flatter overall size histogram. Compare results presented in Fig. 6, for $\eta = 0.8$, with those of Figs. 2 and 5(a), for $\eta = 0.4$.

If small droplets donate mass to large droplets (see Fig. 7), then the 'purple' and the 'overall' histograms shift drastically to the right, as expected.

The importance of the present results lies in the capability of experimentalists nowadays to measure such size histograms [20–23] and thus to conduct experiments under specified controlled conditions that will enable one to verify the general theory and to extract, with the aid of the present theory, submodels for the rate of head-on collisions, the rate of inertial coalescence, and the overall rate of evaporation. A similar effort to measure droplet collision rates in a hollow-cone spray generated by a pressure-swirl atomizer was recently carried out in a pioneering experimental study conducted at NIST by Zurlo *et al.* [24].

In addition, we note that the opposed flow configuration has begun to attract attention for basic experimental and theoretical [25–28] studies of spray

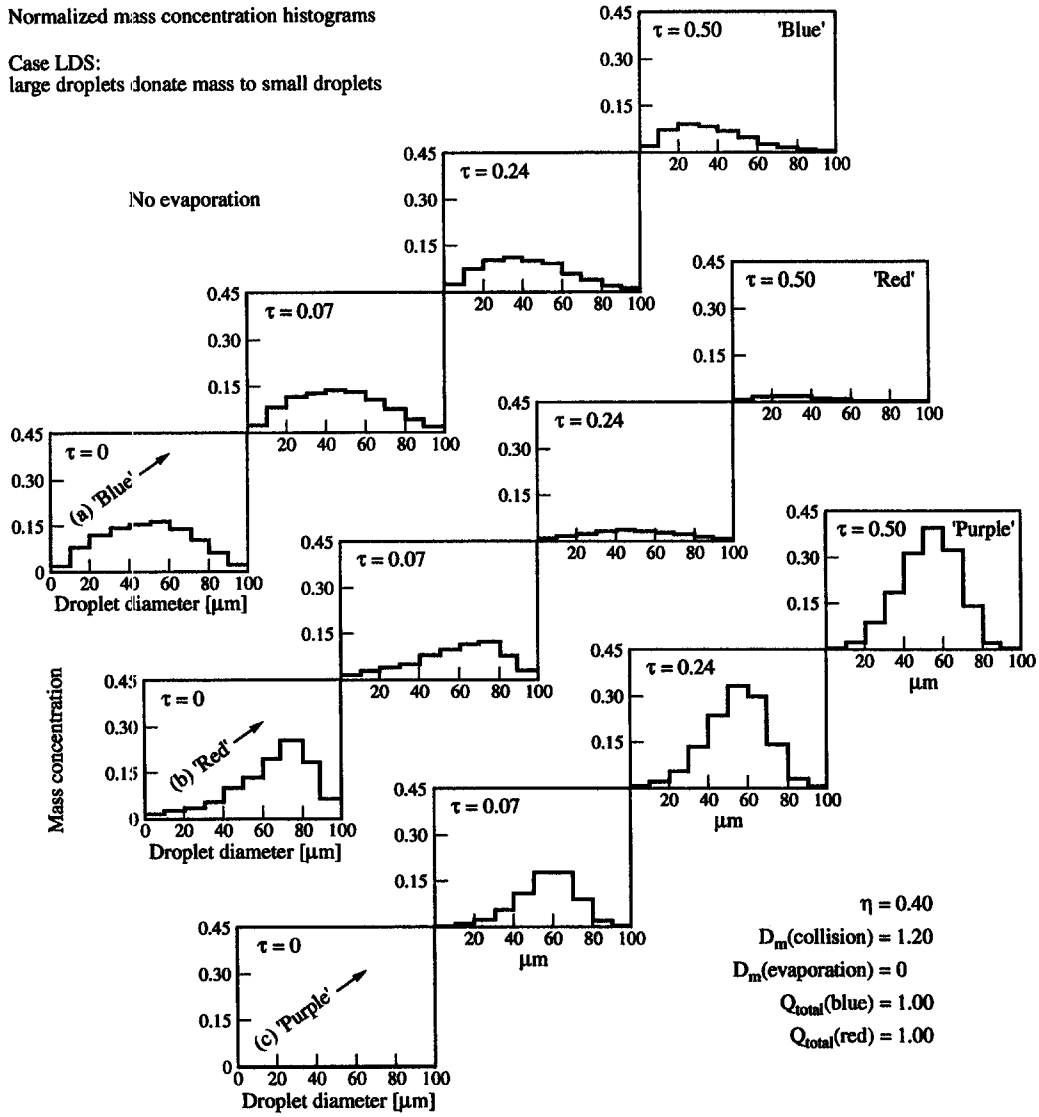

Fig. 2. Time evolution in mass concentrations (given in terms of drop-size histograms) for the 'blue', 'red' and 'purple' sprays due to mass exchange between droplets during head-on collisions, without evaporation; for case LDS, large droplets donate 40% of their mass to small droplets.

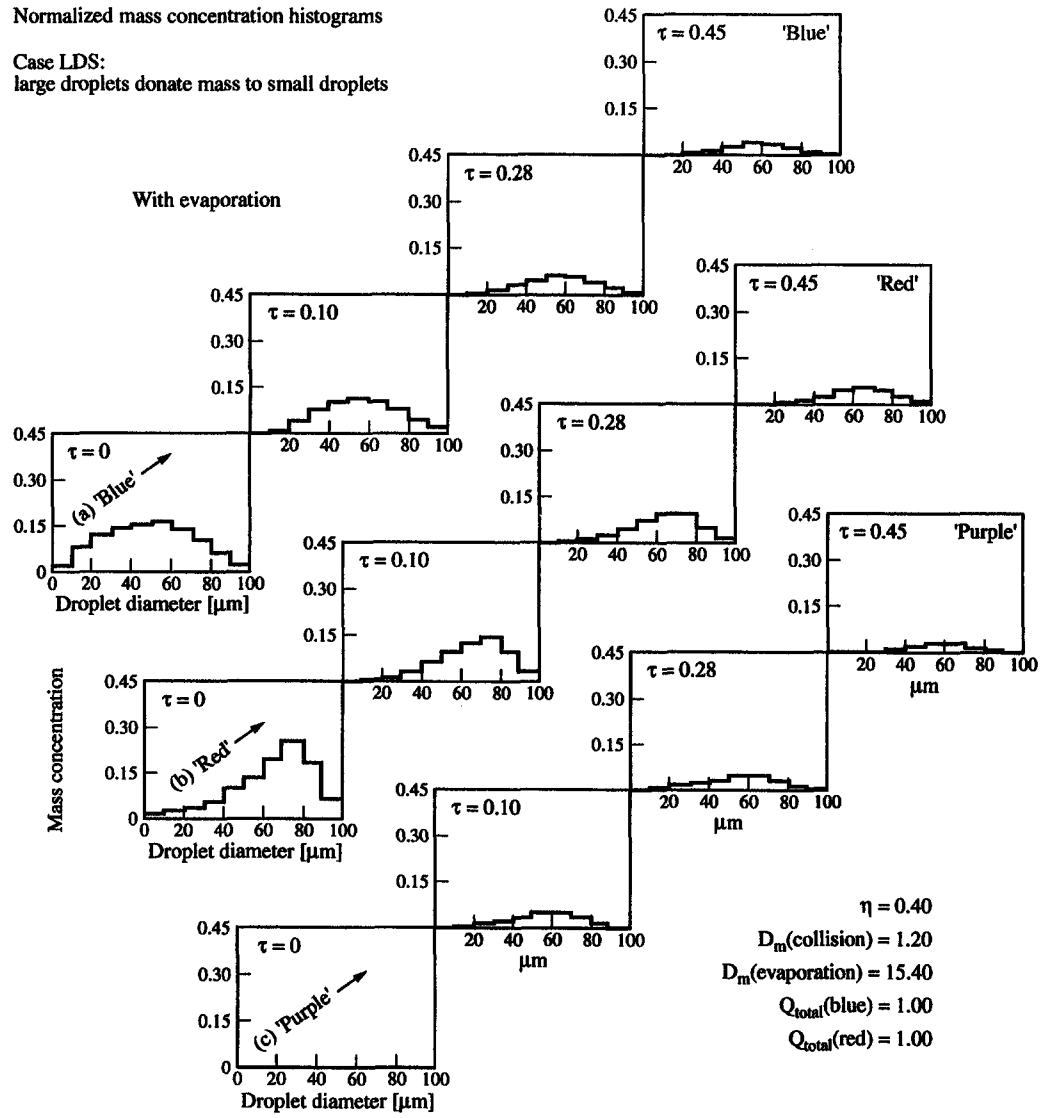

Fig. 3. Time evolution in mass concentrations (given in terms of drop-size histograms) for the 'blue', 'red' and 'purple' sprays due to mass exchange between droplets during head-on collisions, and due to evaporation; for case LDS, large droplets donate 40% of their mass to small droplets.

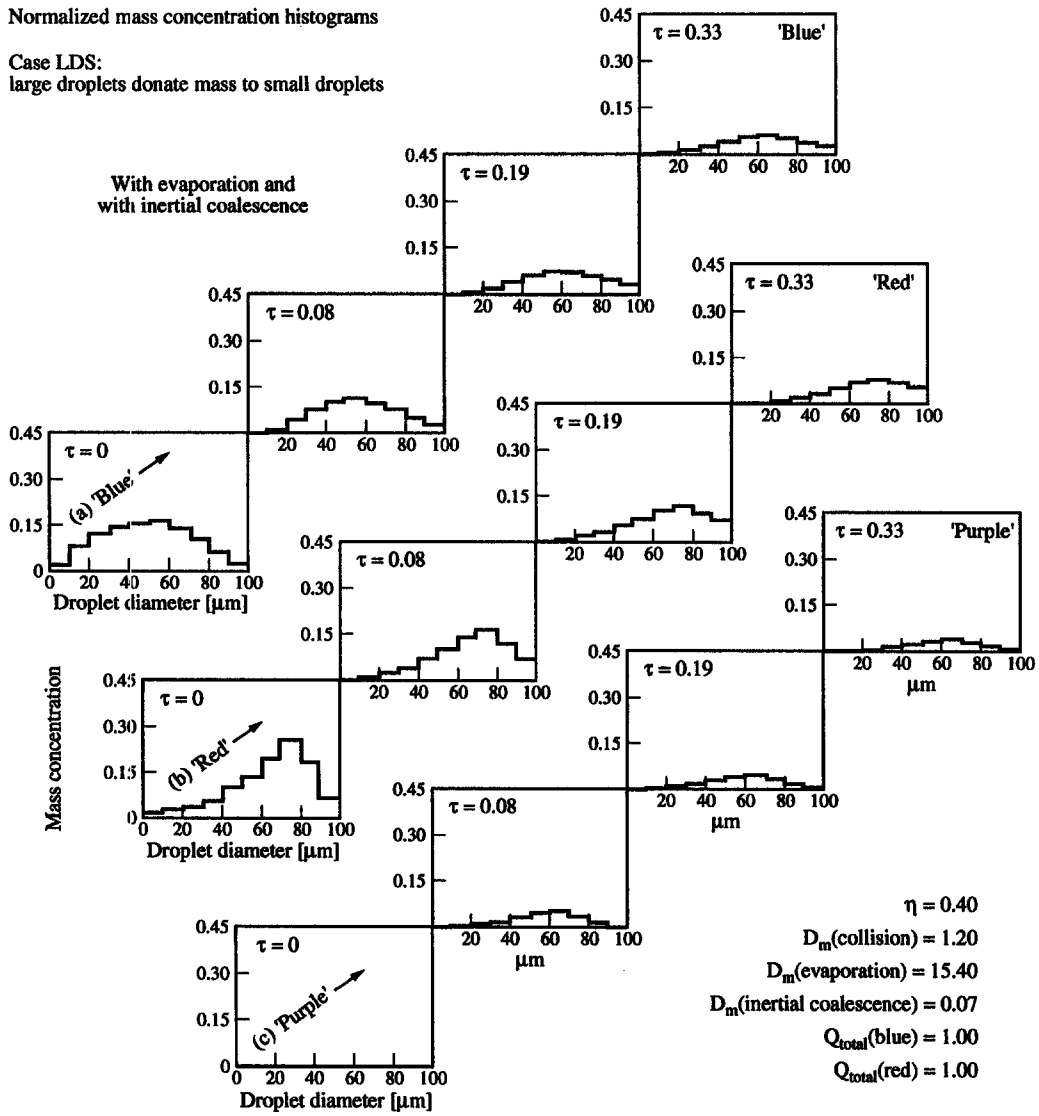

Fig. 4. Time evolution in mass concentrations (given in terms of drop-size histograms) for the 'blue', 'red' and 'purple' sprays due to mass exchange between droplets during head-on collisions, and due to evaporation and inertial coalescence; for case LDS, large droplets donate 40% of their mass to small droplets.

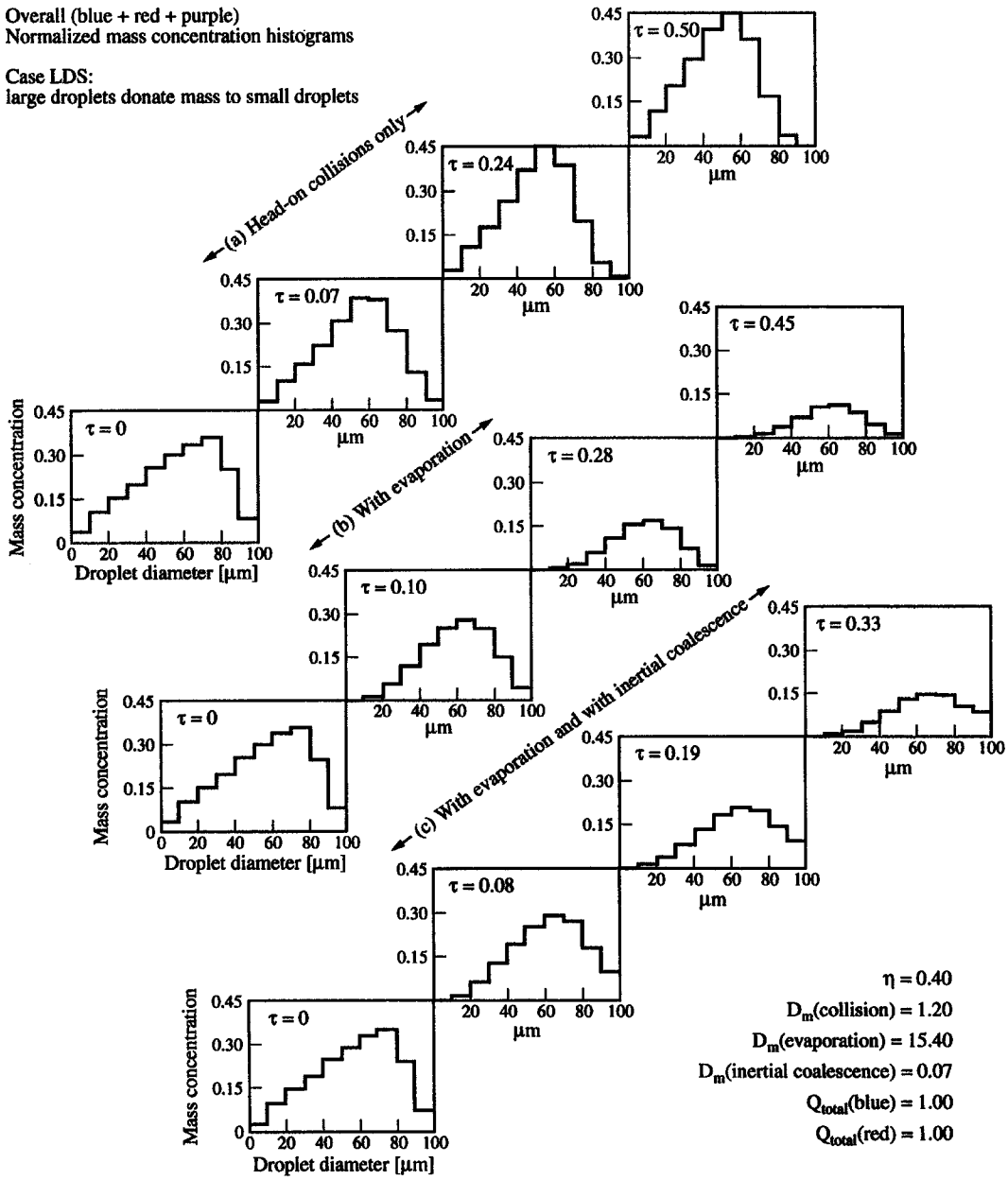

Fig. 5. Comparison of the time evolution in the overall ('blue' + 'red' + 'purple') mass concentrations (given in terms of drop-size histograms) given: (a) head-on collisions only; (b) with evaporation; and (c) with evaporation and with inertial coalescence; for case LDS, large droplets donate 40% of their mass to small droplets.

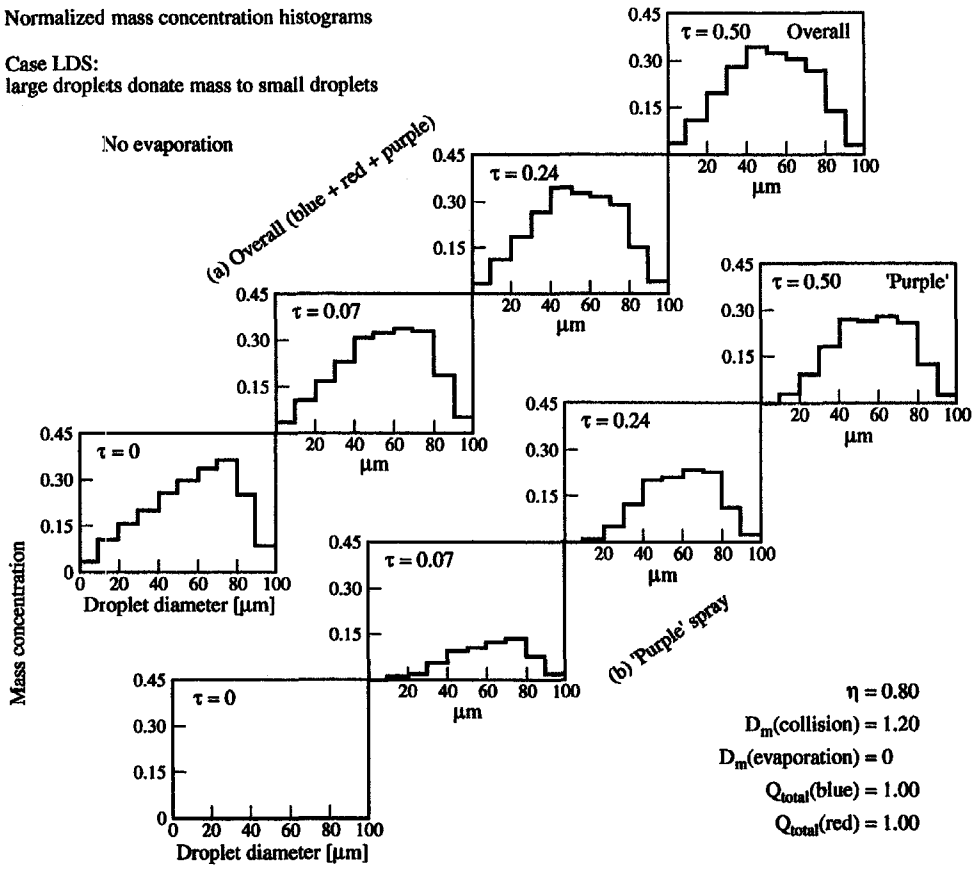

Fig. 6. Time evolution in the 'purple' and the overall ('blue'+'red'+'purple') mass concentrations (given in terms of drop-size histograms) due to head-on collisions only, $\eta = 0.8$; for case LDS, large droplets donate 80% of their mass to small droplets.

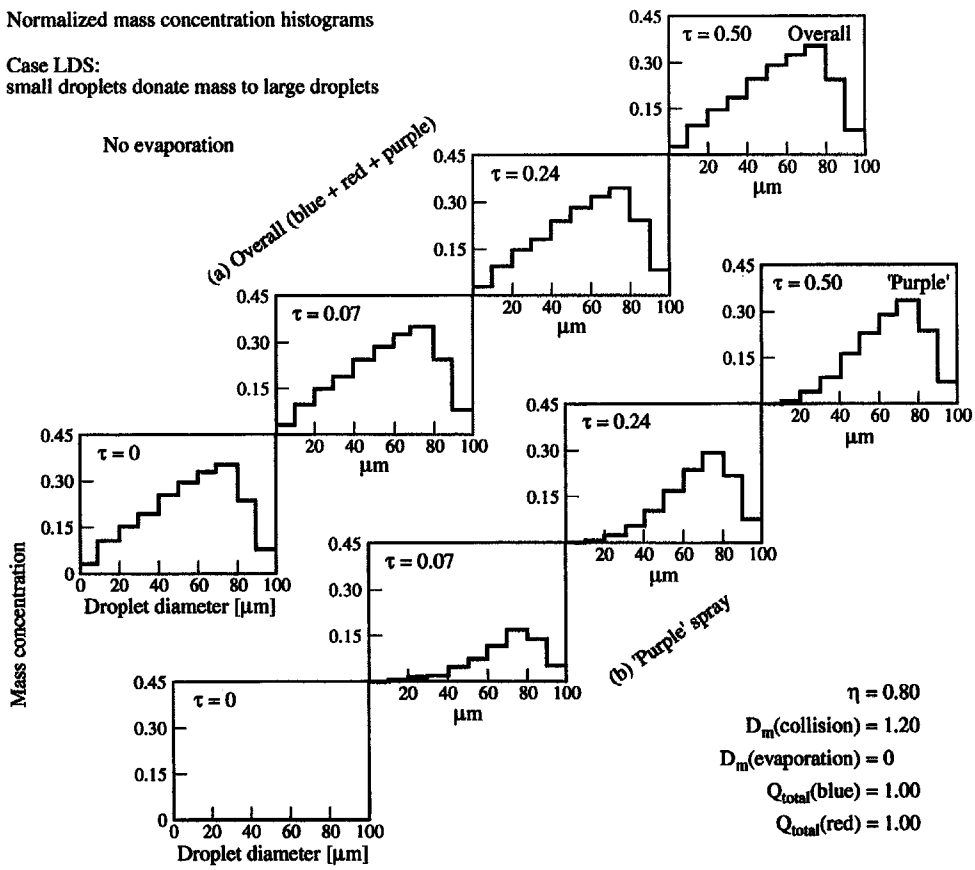

Fig. 7. Time evolution in the 'purple' and the overall ('blue'+'red'+'purple') mass concentrations (given in terms of drop-size histograms) due to head-on collisions only, $\eta = 0.8$; for case SDL, small droplets donate 80% of their mass to large droplets.

combustion, although these have so far been restricted to situations in which the spray of droplets is introduced in one of the opposing jets only. Introduction of a spray of liquid oxidant and/or a second liquid fuel into the second jet will undoubtedly invoke head-on collisions of the sort we have examined here. The conditions for mass transferring head-on collisions in such circumstances can be estimated in terms of the Weber number, which is defined as

$$We = \rho(r_1 + r_2)u^2/\sigma \tag{43}$$

where r_1 and r_2 are the radii of the two colliding droplets, ρ is the fluid density, σ is the surface tension and u is the relative velocity at collision. For collisions between n-heptane and n-octane droplets we note that these hydrocarbon fuels have densities at 400 K of 0.61×10^3 and 0.63×10^3 kg m^{-3}, respectively, whilst their surface tensions are 11.54×10^{-3} and 13.25×10^{-3} N m^{-1}, respectively. Taking head-on collisions between droplets of radii 5 and 100 μm gives a Weber number of about

$$We \approx 5.5u^2. \tag{44}$$

The relevant range of Weber numbers for head-on collisions under which mass exchange occurs in the manner we have analyzed is given by Jiang *et al.* [4] as $0.1 \lesssim We \lesssim 50$ (domains I, II and III of ref. [4]). Substituting these limits into equation (44) leads to a relative velocity at impact in the range $0.135 < u < 3.015$ in units of meters per second. These sorts of velocities occur with those used in the experimental work of Chen and Gomez [25] on laminar counterflow spray flames, so that we foresee our analysis assuming relevance in appropriate modelling of the counterflow combustion set-up. (We also point out that using these data enables us to bracket the size range for the control volume of our analysis. A typical experimentally used value of the strain rate parameter, a, is of the order of 100 s^{-1}. Combining this with the aforementioned range of u leads to a length dimension of the control volume $1.3 \times 10^{-3} \lesssim x \lesssim 3 \times 10^{-2}$ m.)

Finally, we turn to an estimate of the inertial coalescence parameter, $\tau_{\text{inertial coalescence}}$ [equation (42)]. Making use of the maximum values of the (inertial) collision frequency measured by Zurlo *et al.* [24] and the fluid dynamic data we have mentioned in connection

with head-on droplet collisions, leads us to conclude that $\tau_{\text{inertial coalescence}} \ll \tau_{\text{collision}}$ which is in keeping with the sort of collision Damkohler number values we have utilized for our calculations.

4. CONCLUSIONS

New sectional equations for mass exchange between droplets during head-on collisions of multisize (polydisperse) sprays have been presented. Solution of these sectional equations for the following three special cases have been presented: (a) head-on collisions only; (b) with evaporation; and (c) with evaporation and with inertial coalescence. These results indicate the relative contribution of each of the above processes to the evolution in droplet size distribution of the colliding sprays and the newly formed droplets.

REFERENCES

1. N. Ashgriz and J. Y. Poo, Coalescence and separation in binary collisions of liquid drops, *J. Fluid Mech.* **221,** 183–204 (1990).
2. N. Ashgriz and P. Givi, Binary collision dynamics of fuel droplets, *Int. J. Heat Fluid Flow* **8,** 205–210 (1987).
3. N. Ashgriz and P. Givi, Coalescence efficiencies of fuel droplets in binary collisions, *Int. Commun. Heat Mass Transfer* **16,** 11–20 (1989).
4. Y. J. Jiang, A. Umemura and C. K. Law, An experimental investigation of the collision behaviour of hydrocarbon droplets, *J. Fluid Mech.* **234,** 171–190 (1992).
5. J. R. Adam, N. R. Lindblad and C. D. Hendricks, The collision, coalescence, and disruption of water droplets, *J. Appl. Phys.* **39,** 5173–5180 (1968).
6. V. A. Arkhipov, I. M. Vasenin and V. F. Trofimov, Stability of colliding drops of ideal liquid, *Tomsk.*, translated from *Zh. Prikl. Mekh. Tekhn. Fiz.* **3,** 95–98 (1983).
7. P. J. O'Rourke and F. V. Bracco, Modelling of drop interactions in thick sprays and a comparison with experiments, *Stratified Charged Auto Engineering Conference*, pp. 101–116. Institute of Mechanical Engineering (1980).
8. Y. Tambour, Coalescence of vaporizing kerosene fuel sprays in a turbulent jet, *Atomisation Spray Technol.* **1,** 125–146 (1985). See also: Simulation of coalescence and vaporization of kerosene fuel sprays in a turbulent jet: a sectional approach, *AIAA/ASME/ASEE 21st Joint Propulsion Conference*, Monterey, AIAA Paper No. 85-1315 (1985).
9. J. B. Greenberg and Y. Tambour, Far-field coalescence effects in polydisperse spray jet diffusion flames, *Twenty-first Symposium (International) on Combustion*, pp. 655–663. The Combustion Institute (1986).
10. Y. Tambour and J. B. Greenberg, A theoretical study of polydisperse spray diffusion flames in the far-field of a fuel-injector, *Int. J. Turbo-Jet Engines* **10,** 323–332 (1993).
11. Y. Tambour and S. Zehavi, Derivation of near-field sectional equations for the dynamics of polydisperse spray flows: an analysis of the relaxation zone behind a normal shock wave, *Combust. Flame* **95,** 383–409 (1993).
12. A. J. Yule, P. R. Ereaut and A. Ungut, Droplet sizes and velocities in vaporizing sprays, *Combust. Flame* **54,** pp. 15–22 (1983).
13. Y. Tambour, A sectional model for evaporation and combustion of sprays of liquid fuels, *Israel J. Technol.* **18,** 47–56 (1980).
14. J. B. Greenberg, I. Silverman and Y. Tambour, On the origins of spray sectional conservation equations, *Combust. Flame* **93,** 90–96 (1993).
15. I. Silverman, J. B. Greenberg and Y. Tambour, Asymptotic analysis of a premixed polydisperse spray flame, *SIAM J. Appl. Math.* **51,** 1284–1303 (1991).
16. I. Silverman, J. B. Greenberg and Y. Tambour, Solutions of polydisperse spray sectional-equations via a multiple-scale approach: an analysis of a premixed polydisperse spray flame, *Atomization Sprays* **2,** 193–224 (1992).
17. Y. Tambour, Vaporization of polydisperse fuel sprays in a laminar boundary layer flow: a sectional approach, *Combust. Flame* **58,** 103–114 (1984).
18. Y. Tambour, A Lagrangian sectional approach for simulating droplet size distribution of vaporizing fuel sprays in a turbulent jet, *Combust. Flame* **60,** 15–28 (1985).
19. D. Katoshevski and Y. Tambour, A theoretical study of polydisperse liquid-sprays in a free shear-layer flow, *Physics Fluids A* **5,** 3085–3098 (1993).
20. W. D. Bachalo, A. Brena de la Rosa and R. C. Rudoff, Advances in diagnostics for complete spray characterization, *ICLASS-88,* 287–295 (1988).
21. C. F. Edwards and R. C. Rudoff, Structure of a swirl-stabilized spray flame by imaging, laser Doppler velocimetry and phase Doppler anemometry, *Twenty-third Symposium (International) on Combustion*, pp. 1353–1359. Orleans, France (1990).
22. C. Presser, A. K. Gupta, C. T. Avedisian and H. G. Semerjian, Fuel property effects on the structure of spray flames, *Twenty-third Symposium (International) on Combustion*, pp. 1361–1367. Orleans, France (1990).
23. C. Presser, A. K. Gupta and H. G. Semerjian, Aerodynamic characteristics of swirling spray flames: pressure-jet atomizer, *Combust. Flame* **92,** 25–44 (1993).
24. J. R. Zurlo, C. Presser and H. G. Semerjian, Estimation of droplet collision frequency in a spray, *ILASS—Americas—92, Fifth Annual Conference on Liquid Atomization and Spray Systems*, 18–20 May, pp. 97–101. San Ramon, CA (1992).
25. G. Chen and A. Gomez, Counterflow diffusion flames of quasi-monodisperse electrostatic sprays, *Twenty-fourth Symposium (International) on Combustion*, Australia (1992).
26. S. C. Li, P. A. Libby and F. A. Williams, Experimental and theoretical studies of counterflow spray diffusion flames, *Twenty-fourth Symposium (International) on Combustion*, Australia (1992).
27. A. Kitron, T. Elperin and A. Tamir, Monte Carlo simulation of gas–solids suspension flows in impinging stream reactors, *Int. J. Multiphase Flow* **16,** pp. 1–18 (1990).
28. J. B. Greenberg, D. Albagli and Y. Tambour, An opposed jet quasi-monodispersed spray diffusion flame, *Combust. Sci. Technol.* **50,** 255–270 (1986).